IEEE Access
Multidisciplinary | Rapid Review | Open Access Journal

Received 12 July 2024, accepted 15 August 2024, date of publication 19 August 2024, date of current version 30 August 2024.

Digital Object Identifier 10.1109/ACCESS.2024.3446032

RESEARCH ARTICLE

Metaheuristic Algorithm Based Energy Management System for Electric Vehicle Charging Station

JENNIE ANGELA JOSE SHIRLEY, (Student Member, IEEE), R. P. POOJA, AND MADDIKARA JAYA BHARATA REDDY, (Senior Member, IEEE)
National Institute of Technology Tiruchirappalli, Tiruchirappalli 620015, India

Corresponding author: Maddikara Jaya Bharata Reddy (jayabharat_res@yahoo.co.in)

ABSTRACT Electric Vehicles (EVs) are at the forefront of the transition to sustainability. Their almost zero tailpipe emissions and contribution to noise pollution make them suitable for minimizing the current levels of environmental pollution. One aspect that hinders the widespread adoption of EVs is the limited availability of Electric Vehicle Charging Stations (EVCS) in remote areas, making the charging costs extremely high. The goal of reducing EV charging cost can be achieved by integrating renewables into a conventional power system. This study proposes a method for optimizing the charging cost by utilizing renewable energy resources for an EVCS in a modified IEEE 33 bus system. This study involves the incorporation of three renewable energy sources: solar, wind and biogas. Energy management between the various sources and the EVCS was achieved through a metaheuristic algorithm-based Energy Management System (MAEMS). The proposed MAEMS was used to develop a dynamic pricing scheme. A techno-economic analysis of the system was conducted. The analysis was performed on the MATLAB-Simulink platform, considering the standards of the Indian EVCS system.

INDEX TERMS Electric vehicle charging stations, energy management system, metaheuristic algorithms, renewable energy sources.

I. INTRODUCTION

The increasing dependence on fossil fuels to meet the ever-growing demand for electricity has led to long-lasting deteriorating effects on the environment [1]. This has subsequently resulted in poor quality of life and chronic illnesses in children and adults alike [2]. Under such circumstances, the introduction of renewable, eco-friendly, and non-exhaustible energy sources has proven to be a great choice.

With regard to growing concerns about fossil fuels, the transition to Electric Vehicles (EVs) over their fossil fueled counterparts is preferred [3]. Vehicular electrification enables an effective transition to a sustainable and zero-carbon emission environment. Similar to the case of fossil fueled Internal Combustion Engine (ICE) vehicles, EVs require evenly distributed Electric Vehicle Charging Stations (EVCS), with proper planning of the location and capacity [4].

Furthermore, the charging duration and cost must be minimized for EVs to be a better selling commodity [5]. This necessitates an intelligent energy management system (EMS) that would help in the optimal allocation of resources to the components of the power system and in presenting a more economical pricing scheme for EV users.

EMS for EVCS has been extensively studied worldwide [6]. Resource allocation and cost optimization are problems that have gained recognition. These problems need to be addressed to enable the safe, reliable, and economical operation of power systems with EVCS and renewables.

An EMS for a residential EVCS with a photovoltaic (PV) power source and energy storage system (ESS) was proposed in [7]. Real-time coordination between the PV power station, grid and the ESS was implemented, thereby enabling the

The associate editor coordinating the review of this manuscript and approving it for publication was Chandan Kumar.

EVCS to function as a stand-alone system. This study did not consider the different types of charging available to the EVs.

The optimal configuration and techno-economic assessment for a solar-powered EVCS were analyzed for four Indian cities with varied solar conditions in [8]. The environmental benefits of the proposed system are also evaluated.

An EMS for public EVCS integrated with a community microgrid was proposed in [9], based on the switching mechanism from one trading market to another. The EMS minimizes the charging costs and satisfies the community load. However, the environmental footprint of the proposed model has not been assessed.

A dynamic EMS for an integrated solar and energy storage charging station, based on a real-world situation in Taiwan was developed in [10]. The proposed EMS optimized the economic efficiency of the EVCS. However, this study considers only the EVCS for fast charging.

A biogas–solar powered EVCS was proposed for a typical location in Karnataka in [11]. Techno-economic and environmental assessments were also conducted. It was observed that dependency on the grid reduced with improved environmental benefits in terms of carbon dioxide emissions.

A grid connected PV battery system was proposed and analyzed using HOMER to check both the economic and technical feasibility of the model in [12]. A system with reduced charging costs was developed. Different patterns and trends in EV charging were not considered in this analysis.

The authors of [13] proposed a fuzzy-logic based approach to develop a method for charging priority identification, considering parameters such as the battery state of charge (SOC), charging cost, peak power demand, and waiting time. This model aims to benefit both the utility and EV users.

A hybrid biogas and solar grid-connected EVCS system with residential loads in Bangladesh was analyzed using MATLAB-Simulink in [14] and optimized using a fuzzy logic-based algorithm. A high level of expertise is required to develop a fuzzy-based model for complex power distribution systems.

A hybrid generation system comprising of two or more unreliable and intermittent energy sources can provide better system reliability. Wind and solar power have complementary energy generation profiles; thus, the installation of a hybrid solar-wind energy system would ensure a high efficiency and stable power supply [15], [16]. A techno-economic assessment of a hybrid solar-wind system, single solar PV system, and single wind system was developed in [17]. It was concluded that the hybrid system is more economical and has a better system performance than either of the single systems.

The existing literature does not mention wind, solar and biogas system-based EVCS. Furthermore, the use of metaheuristic methods for optimization would make the system more robust and reliable. This study proposes an metaheuristic algorithm-based Energy Management System (MAEMS) for power systems with an EVCS. The major contributions of this study are as follows:

[1] A modified IEEE 33 bus system with a wind farm, a solar PV system and biogas plant with EVCS was developed.
[2] Alternating Current (AC) and Direct Current (DC) charging were considered in the EVCS, which was developed according to Indian standards.
[3] MAEMS is implemented using three metaheuristic algorithms: Artificial Bee Colony (ABC), Social Group Optimization (SGO), and Particle Swarm Optimization (PSO). The results were compared with those obtained using the non-linear solver.
[4] The dynamic pricing scheme obtained was compared with the conventional time-of-day grid tariff.
[5] Techno-economic assessment of the developed model is made.

Figure 1 presents the components of this study. The following section provides an overview of the EMS and metaheuristics.

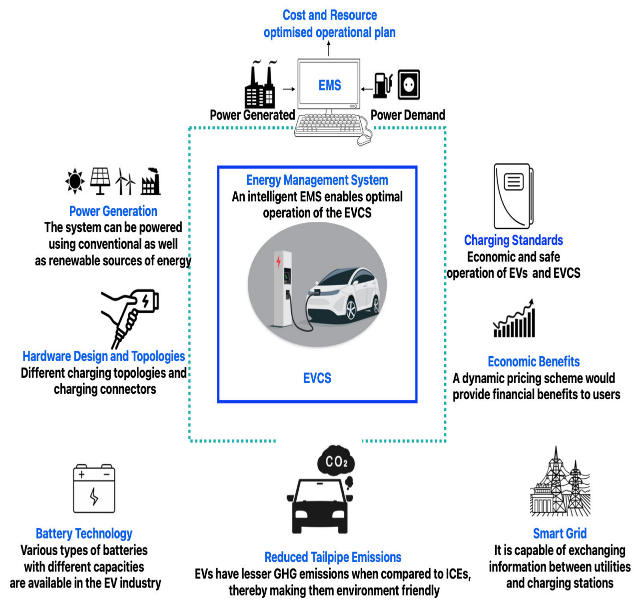

FIGURE 1. Components of the Study.

II. THEORETICAL BACKGROUND

The availability of limited energy resources necessitates the proper management and utilization of resources. Ensuring a balance between power generation and consumption, that is, energy management, would help maintain a reliable power system [18]. An Energy Management System (EMS) enables the reliable, efficient, and economic operation of a power system by considering the generated power, status of various components, forecasted load, weather, and cost of energy generation. An EMS can thus be enlisted to arrive at solutions for single or multi-objective functions such as monitoring real and reactive power, minimizing operational costs, minimizing losses, and energy balancing in transmission systems [19].

The Supervisory Control and Data Acquisition (SCADA) system collects real time data from equipment in remote locations, and controls them based on specified constraints. Intelligent Electronic Devices (IEDs) are present in the field. They can be sensors or actuators. The sensors obtain data from the equipment, whereas the actuators implement the control mechanism decided by the central controller. Remote Terminal Units (RTUs) collect data from sensors and send them to the central controller, that is, the SCADA master unit. Programmable Logic Controllers (PLCs) collect decisions from the central controller and send them to the actuators to control the respective equipment [20], [21]. RTUs measure data once every 4-10s [22].

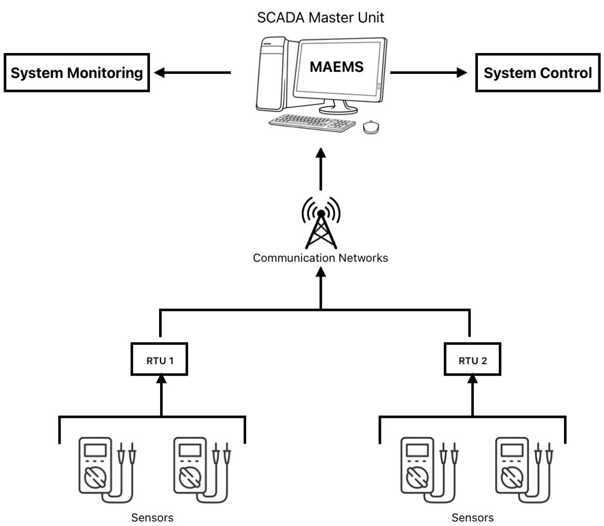

FIGURE 2. Supervisory control and data acquisition system.

Figure 2 shows a typical SCADA system. Different sensors collect real-time information, that is sent to the RTUs connected to them. Through communication networks, the information reaches the SCADA master unit, where decisions are made to control and monitor the system. This helps to prevent and mitigate faults in the power system, thereby ensuring its safe operation. The developed MAEMS works using an SCADA system, with voltage and current sensors available at each node.

For EMS, in the SCADA control center, we require a dedicated algorithm that can manage the system with the given constraint for a reduced cost. Mathematical programming is a classical optimization technique in which one or more objective functions are optimized based on a set of constraints. Mathematical programming methods include non-linear, linear, second-order conic and mixed-integer programming. Although they can reach a global optimum, they lack efficiency owing to the high computational effort required when compared to metaheuristics. Furthermore, the optimization process is time consuming and cannot be adopted for complex systems with a large number of variables [23], [24].

The metaheuristic model is a well-known and higher-level method used to find the best solution to complex optimization problems. It falls under the category of stochastic optimization. Often, this method is preferred over other conventional iterative techniques, optimization algorithms, and simple heuristics because of its practical efficacy and reduced computational efforts. Different algorithms in metaheuristics are designed based on ideas that exist in nature. Some of the commonly used models in population–based metaheuristics are the Genetic Algorithm (GA), Artificial Bee Colony (ABC), Particle Swarm Optimization (PSO), Gravitational Search Algorithm (GSA), and Spotted Hyena Optimizer (SHO). These techniques have found applications in a wide range of industries, from artificial intelligence and the Internet of Things to engineering design because of their proven efficiency and robustness [25].

In this study, a MAEMS was designed to minimize the charging cost for consumers and maximize renewable energy utilization. MAEMS optimizes the problem based on the real-time situation of the various parameters involved. The following section elucidates the proposed energy-management algorithm for optimization.

III. MAEMS ALGORITHM

A MAEMS was developed for a modified IEEE 33 bus system with EVCS. The MAEMS achieves its objectives by considering the generated power, power demand, charging time of the EV, and the base tariff. All the resources considered are assumed to be owned and operated by the utility. The utility takes care of the relationship between the consumer and the supply side.

The following constraints are observed during the design of the system:

- The voltage (V) range lies within the specified lower V_{ll} (0.95 pu) and upper V_{ul} (1.05 pu) limits. The rated line-to-line voltage of the system was 415 V.

$$V_{ll} < V < V_{ul} \tag{1}$$

- The frequency (f) was always maintained within the fixed lower f_{ll} (49.5 Hz) and upper f_{ul} (50.5 Hz) limits. The rated frequency of the system is 50 Hz.

$$f_{ll} < f < f_{ul} \tag{2}$$

- The line limits are always followed, that is, the current flowing through the transmission lines (I_{line}) should be less than or equal to the rated current (I_{rated}).

$$I_{line} \leq I_{rated} \tag{3}$$

MAEMS aims to minimize the charging cost (C_c) and maximize renewable energy utilization (U_{RES}). The EV user benefits from the developed dynamic pricing scheme. The objective functions can be defined as

$$\min(C_c) \text{ and } \max(U_{RES}) \tag{4}$$

First, the power demand from the EVCS ($P_{d,EVCS}$) is calculated as

$$P_{d,EVCS} = \sum_{i=1}^{n} P_i \tag{5}$$

where P_i denotes the power demand of the i^{th} EVCS connected to the system.

The total power demand in the system ($P_{d,total}$) is given by

$$P_{d,total} = P_{d,EVCS} + \sum_{j=1}^{m} P_{load,j} + P_{tr.losses} \tag{6}$$

where $P_{load,j}$ denotes the power demand of each load connected to the system and $P_{tr.losses}$ represents the transmission losses in the system.

The SOC of the EV battery was constantly monitored to ensure that the battery did not enter unhealthy cycles of overcharging or deep discharging. The power demand of an EV depends on the SOC of the battery, and a battery with a higher SOC has a lower power demand.

$$20\% \leq SOC \leq 80\% \tag{7}$$

The charging duration is an important parameter for optimizing the cost, as it is another indicator of the power demand from the perspective of the EVCS.

The renewable power generated ($P_{gen,ren}$) is evaluated as the sum of the generations from the solar PV system, wind farm, and the biogas plant, and can be expressed as

$$P_{gen,ren} = \sum_{t=1}^{n} (P_{PV,t} + P_{wind,t} + P_{biogas,t}) \tag{8}$$

where, $P_{PV,t}$, $P_{wind,t}$ and $P_{biogas,t}$ indicate the power generated by the solar PV system, the wind farm and the biogas plant at time 't', respectively.

A. MAXIMIZATION OF RENEWABLE ENERGY UTILIZATION

The power generated from renewables, together with the power from the grid, was used to provide power to the system. When the power generated by renewables exceeds the power demand, no power is drawn from the grid. In contrast, when the generated renewable power is less than the total power demand, a deficit is provided by the grid. The power drawn from the grid (P_{grid}) is given by

$$P_{grid} = \begin{cases} 0, & \text{if } P_{gen,ren} = P_{d,total} \\ P_{d,total} - P_{gen,ren}, & \text{if } P_{gen,ren} \neq P_{d,total} \end{cases} \tag{9}$$

If the power generated from the renewable power sources exceeds the power demand, the excess is fed back to the grid. The Renewable Energy Utilization (%RE) was calculated as a percentage of the power contribution of the renewable sources when compared to the total power obtained.

$$\%RE = \frac{P_{gen,ren}}{P_{gen,ren} + P_{grid}} \times 100 \tag{10}$$

B. MINIMIZATION OF CHARGING COST

The charging costs in the developed dynamic pricing scheme depend on the power demand and generation. The power obtained from two renewable sources, namely, the solar PV system and the wind farm was checked. Their per unit costs were calculated based on their respective generations. The pseudocode for developing a dynamic pricing scheme is presented in Algorithm 1.

Algorithm 1 Dynamic Pricing Scheme

Input:
Total Power Demand $(P_{d,t})$
Renewable Power Generated (Pen,ren)
Cost per kWh (Solar PV System - S_1, S_2, S_3;
Wind farm $-W_1$, W_2, W_3)
Generated Power (Solar PV system P_{solar}, Wind farm P_{wind})
Lower limits $-P_{solar,1}$, $P_{wind,1}$
Upper limits $-P_{solar,u}$, $P_{wind,u}$
Output: Optimised charging cost and dynamic pricing scheme
Initialization: Set the initial charging cost as zero
Compute total power demand in the system for a time instant 't' according to equation (6)
Calculate the total renewable power generated at time 't' according to equation (8)
If $P_{solar} \leq P_{solar,1}$, **do**
  PV Cost $= S_1$
elseif $P_{solar,1}, < P_{solar} < P_{solar,u}$ **do**
  PV Cost $= S_2$
else do
  PV Cost $= S_3$
end (If loop)
If $P_{wind} \leq P_{wind,1}$ **do**
  Wind Cost $= W_1$
elseif $P_{wind,1} < P_{wind} < P_{wind,u}$ **do**
  Wind Cost $= W_2$
else do
  Wind Cost $= W_3$
end (If loop)
If $P_{gen,ren} \geq P_{d,t}$ **do**
  Dynamic Price calculation based on per unit cost of renewable sources
Else do
  Dynamic Price calculation based on per unit cost of renewable sources and grid tariff
end (If loop)
end

The generation from renewables is compared with the demand. If the power obtained from renewable energy sources is greater than or equal to the demand, then the per-unit charging cost is determined from the costs of the renewable sources. However, if the renewable sources are unable to meet the power demand, the grid tariff and the respective per -unit cost of the renewables at that instance of

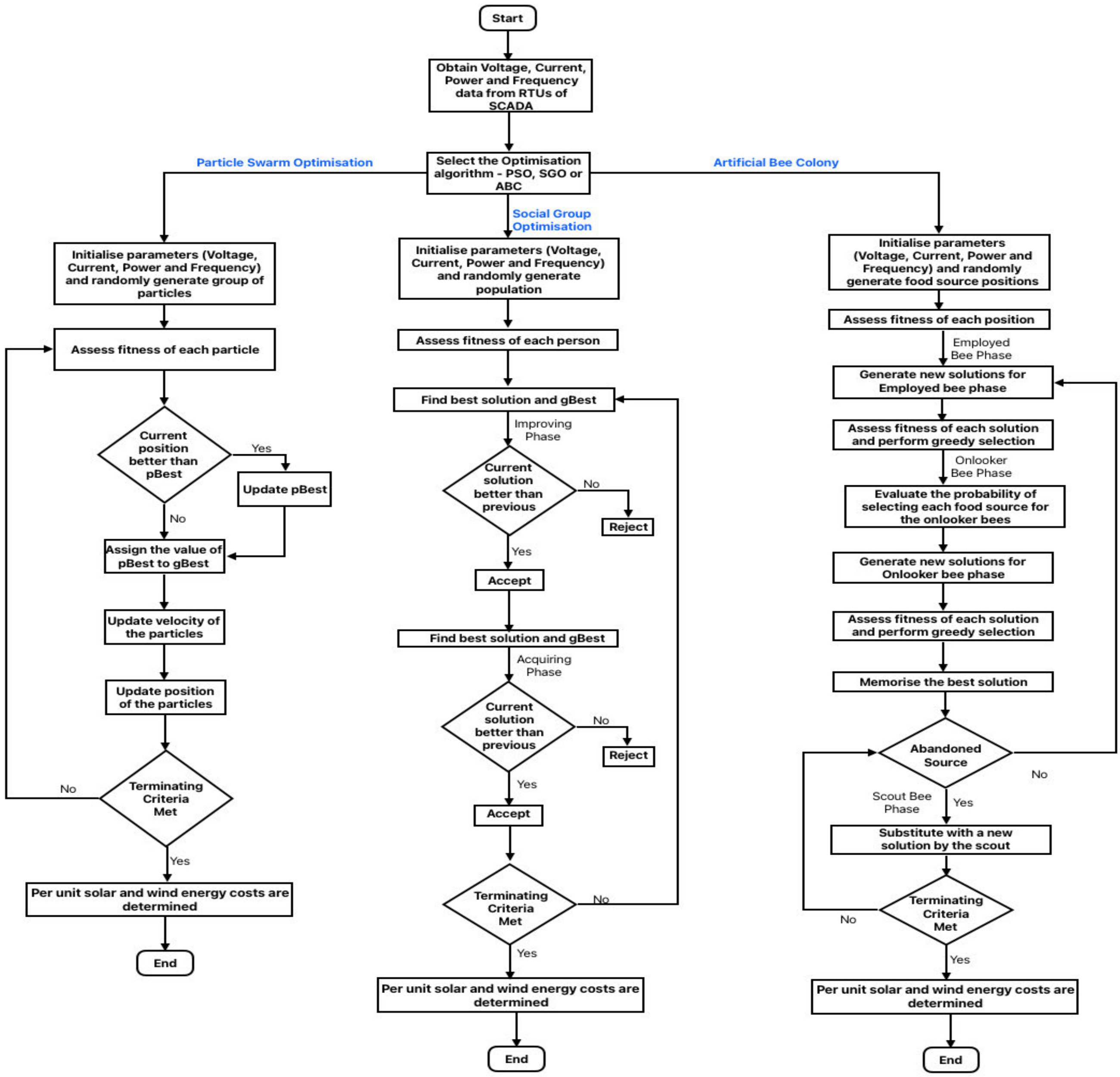

FIGURE 3. Metaheuristic algorithms for minimizing charging cost in modified IEEE 33 bus system.

time are considered. The dynamic pricing scheme provides a constant per kilowatt hour (kWh) cost every hour.

Three metaheuristic algorithms, namely, Artificial Bee Colony (ABC), Social Group Optimization (SGO), and Particle Swarm Optimization (PSO) are used to determine the dynamic pricing scheme. These optimization techniques have better computational efficiency than non-linear programming, which has also been analyzed. The voltage, frequency, power and current data from the different IEDs were used in the SCADA master unit as the input for the MAEMS algorithms. The constraints for each of these electrical parameters are also considered. The per-unit costs of the solar PV system and wind farm vary depending on the individual power generation, as depicted in Algorithm 1. These costs are determined using metaheuristic algorithms, as shown in Figure 3.

1) PARTICLE SWARM OPTIMIZATION (PSO)

PSO is a stochastic optimization method based on the swarm behavior of herds, fish, insects, and birds. In this technique, each potential solution is a particle, with the position and velocity as attributes. The particles in the swarm change their positions based on their learning experience. Thus, the relative position of the particles is updated from one iteration to the next and gradually converges to the optimum value. Each particle has a personal best position (**pBest**), and each swarm has a global best position (**gBest**) [26], [27].

The velocity of particle 'n' during the iteration 'm' ($\mathbf{v_n^m}$) is given by

$$\mathbf{v_n^m} = \mathrm{w}\mathbf{v_n^{m-1}} + \mathrm{c_1}\mathbf{r_1}\left(\mathbf{pBest_n^{m-1}} - \mathbf{x_n^{m-1}}\right) + \mathrm{c_2}\mathbf{r_2}\left(\mathbf{gBest^{m-1}} - \mathbf{x_n^{m-1}}\right) \tag{11}$$

where 'w' is the inertia weight used to balance the global and local exploration, 'c_1' and 'c_2'are acceleration coefficients and '$\mathbf{r_1}$' and '$\mathbf{r_2}$' are random vectors evenly distributed in the range [0, 1].

The position of particle 'n' during the iteration 'm' ($\mathbf{x_n^m}$) can be given by

$$\mathbf{x_n^m} = \mathbf{x_n^{m-1}} + \mathbf{v_n^m} \tag{12}$$

2) SOCIAL GROUP OPTIMIZATION (SGO)

SGO is based on the group solving abilities of humans, which are superior to those of individual problem solving. In the improving phase, each person's knowledge is honed with the influence of the best person (**gBest**) in the group [28]. The updating for person 'n' for the dimension 'm' ($\mathbf{Xnew_n^m}$) is given as

$$\mathbf{Xnew_n^m} = \mathrm{c} \cdot \mathbf{Xold_n^m} + (\mathrm{r} \cdot (\mathbf{gBest} - \mathbf{Xold_n^m})) \tag{13}$$

where 'c' is the self-introspection parameter that lies between 0 and 1 and 'r' is a random number between 0 and 1. '**Xnew**' is accepted if it gives a better fitness than the older value '**Xold**'.

In the acquiring phase, a person in the group ($\mathbf{X_n}$) interacts and learns from the best person and from others who have better knowledge ($\mathbf{X_r}$), such that

$$\mathbf{Xnew_n^m} = \mathbf{c} \cdot \mathbf{Xold_n^m} + \left(\mathrm{r_1} \cdot \left(\mathbf{X_n^m} - \mathbf{X_r^m}\right)\right) + (\mathrm{r_2} \cdot (\mathbf{gBest} - \mathbf{X_n^m})) \tag{14}$$

where 'r_1' and 'r_2' are random number sequences between 0 and 1, respectively. '**Xnew**' is accepted if it gives a better fitness than the older value '**Xold**'. In this phase, a person gains knowledge from members who are more knowledgeable through random interactions.

3) ARTIFICIAL BEE COLONY (ABC) ALGORITHM

The ABC algorithm is based on the foraging behavior of bees. There are three types of honeybees, employed bees, onlooker bees, and scout bees. The employed bees search for food around the source stored in their memory and provide information about the sources to the onlooker bees. Onlooker bees evaluate and select suitable food sources. Scout bees arise from a few employed bees who abandon their food sources and search for new ones [29].

Each employed bee 'x_n' in the swarm 'X_n' generates a new solution ($\mathbf{v_n^m}$) in the vicinity of its present position as given by

$$\mathbf{v_n^m} = \mathbf{x_n^m} + \emptyset_n^m \cdot \left(\mathbf{x_n^m} - \mathbf{x_k^m}\right) \tag{15}$$

where '$\mathbf{x_k}$' is a random solution, 'm' is a random dimension index and '$\emptyset$' is a random number in the range [−1, 1]. After the solution set '$\mathbf{V_n}$' is obtained, a greedy selection is performed. If the fitness of '$\mathbf{V_n}$' is better than that of '$\mathbf{X_n}$', '$\mathbf{X_n}$' is replaced by '$\mathbf{V_n}$'.

If a food source is abandoned, it is replaced with '$\mathbf{X_n}$' given by

$$\mathbf{x_n^m} = \mathrm{lb_m} + \mathrm{rand}(0, 1) \cdot (\mathrm{ub_m} - \mathrm{lb_m}) \tag{16}$$

where rand (0,1) is a random number between 0 and 1, and lb, ub are the lower and upper bounds of dimension 'm'.

MAEMS was implemented on a modified IEEE 33 bus system, as described in the following section.

IV. TEST BED SYSTEM

This study was conducted using a modified IEEE 33 bus system. The EVCS and renewable sources are appended to the system. The MAEMS was developed using the MATLAB Simulink platform. The voltage and current sensors connected to each node gather data from the loads and generators and send them to the SCADA master unit via the RTUs. The MAEMS in the SCADA master unit optimizes this problem.

A. MODIFIED IEEE 33 BUS SYSTEM

An IEEE 33 bus system is used as the base [30]. The system voltage, frequency and line parameters were altered to match the Indian standards [31], [32]. Renewable sources are incorporated into the system. The grid at node 1 is considered to be a swing bus rated at a 415 V line-to-line and 50 Hz frequency. A graphical representation of the modified system is shown in Figure 4.

A wind farm rated at 30 kW was located on bus 11. The output power of the wind farm is proportional to its wind speed. The nominal and maximum wind speeds were considered to be 13.5 m/s and 15 m/s, respectively. A solar PV system rated at 35 kW was made available at bus 18. The rated output power was obtained at an irradiance of 1000 W/m^2 and temperature of 25°C. The irradiance profile varied throughout the day, with the maximum value being obtained at noon. The irradiance fell to zero before sunrise and after sunset.

A biogas plant rated at 45 kW was placed on bus 25. The output of the biogas plant was considered constant throughout the 24 hour period in this study. Three loads were part of the system. Representative of all possible loads in a practical system, they are positioned at nodes 3, 6 and 33 and are rated at 12 kW, 1 kW and 7 kW respectively. The peripherals attached to the respective nodes of the system are presented in Table 1.

Three EVCSs were considered at nodes 2, 19, and 20. The locations are selected based on [33], which proposes the optimal locations for the placement of the EVCS in an

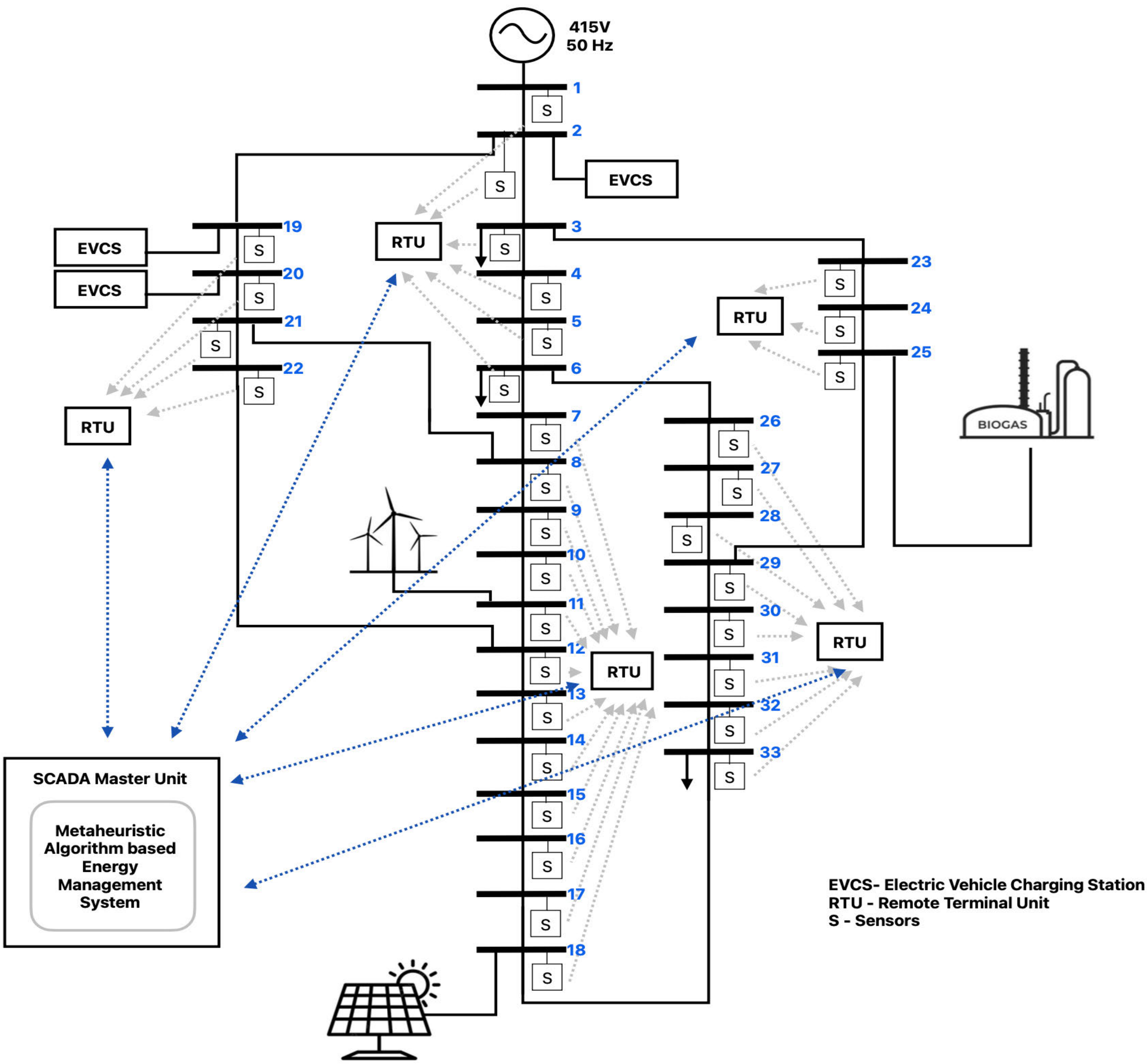

FIGURE 4. Graphical representation of modified IEEE 33 bus system with implementation of MAEMS.

TABLE 1. Peripherals in the modified ieee 33 bus system.

Node	Component	Specifications
2	EVCS	AC – 3×3.3 kW
3	Load	12 kW
6	Load	1 kW
11	Wind Farm	30 kW
18	Solar PV system	35 kW
19	EVCS	AC – 2×21 kW DC – 2×15 kW
20	EVCS	AC – 7.3 kW
25	Biogas Plant	45 kW
33	Load	7 kW

IEEE 33 bus system based on the voltage sensitivity factor (VSF), voltage stability index (VSI), and ampacity limit. The EVCSs at nodes 2 and 20 provide for AC charging, whereas those at node 19 provides consumers with both AC and DC charging.

EVs that may be charged via AC charging are equipped with an onboard charger, which converts the AC power from the grid to DC. However, the DC fast charger, houses the converter within it enabling the EV batteries to be directly charged by it. AC charging is more economical than DC charging. EVCSs are designed for specific power ratings and the time to full charge depends on the SOC of the connected EV battery and the voltage rating of the battery. The maximum current that can be drawn from the AC EVCS is 15 A and that from DC EVCS is 200 A, based on Indian standards [32], as specified in Table 2.

TABLE 2. Specifications of evcs in india.

Type	Power Input	Specification of output	Power Output
AC	3 phase 415 V	15 A 230 V single phase AC	3×3.3 kW
DC	3 phase 415 V AC	200 A 48/60/72 V	15 kW (max)

B. PROPOSED TARIFF STRUCTURE

A dynamic pricing scheme is proposed based on the availability of renewable sources. The higher the renewable generation, the lower is the price specified for the respective source. Because the biogas plant has the same generation throughout the day considered, its per-unit cost, in rupees (Rs.) is fixed, and is considered as Rs. 6.875. The per-unit costs of the solar PV system (S_1, S_2 and S_3) and wind farm (W_1,W_2 and W_3) in Algorithm 1 were optimized using metaheuristic algorithms. The lower and upper bounds assumed for the cost of renewable sources are presented in Table 3, as per Indian standards [34].

TABLE 3. Bounds for optimization.

Source	Power Range	Optimized Cost (Rs./kWh)	Lower Bound (Rs./kWh)	Upper Bound (Rs./kWh)
Solar PV System	$P_{solar} \leq 15$ kW	S_1	2.475	2.66
	15 kW < $P_{solar} < 30$ kW	S_2	2.475	
	$P_{solar} \geq 30$ kW	S_3	2.29	2.475
Wind System	$P_{wind} \leq 10$ kW	W_1	2.615	2.7
	10 kW < $P_{wind} < 20$ kW	W_2	2.615	
	$P_{wind} \geq 20$ kW	W_3	2.53	2.615

The Time of Day (TOD) tariff, as given in [35] is considered the grid tariff, as shown in Table 4.

TABLE 4. Time of day grid tariff.

Time Slot	Energy Charges (Rs./kWh)
0:00 to 5:00 hours	6.03
5:00 to 6:00 hours	6.35
6:00 to 9:00 hours	7.62
9:00 to 18:00 hours	6.35
18:00 to 21:00 hours	7.62
21:00 to 22:00 hours	6.35
22:00 to 24:00 hours	6.03

V. RESULTS AND DISCUSSION

The proposed MAEMS algorithm for the EVCS was implemented in the modified IEEE 33 bus system in the MATLAB Simulink platform. The simulation was performed for a duration of 24 hours, that is, a day, and the variations in the connected EVs and output of the sources were considered accordingly. The results are discussed below.

A. SOURCES

A solar PV system, wind farm and biogas plant were present in the system as mentioned in Section IV. The power generated from each renewable energy source is shown in Figure 5, and the total renewable power generation is shown in Figure 6 (Step 5, Algorithm 1).

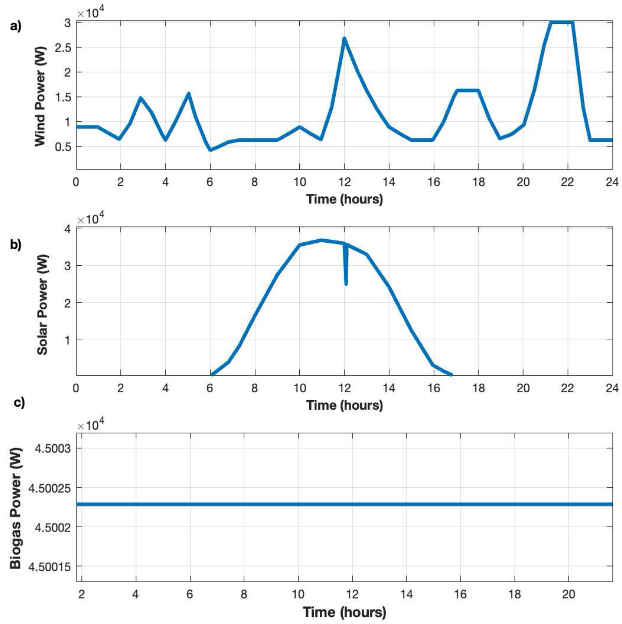

FIGURE 5. Power obtained from a) Wind Farm b) Solar PV System c) Biogas Plant.

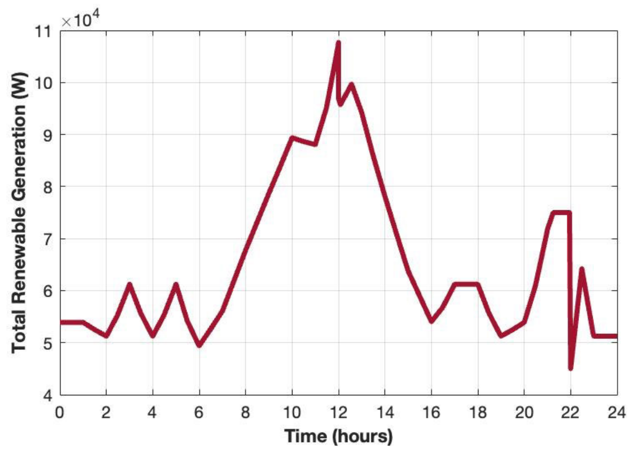

FIGURE 6. Total power obtained from renewable sources.

From Figure 5, it can be observed that the wind profile is dynamic and varies with time. The generated solar power depended on the available solar irradiance. Here, solar irradiance and hence, solar power, is absent from 0 to 6 hours and 17 to 24 hours. The generated solar power reached its peak value around 11 hours. The output from the biogas plant was constant throughout the considered 24 hour period. Thus, the total renewable power generated is dynamic in nature, with a maximum at noon.

B. POWER DEMAND

Figure 7 shows the number of EVs connected to the system, which is used for the proposed work.

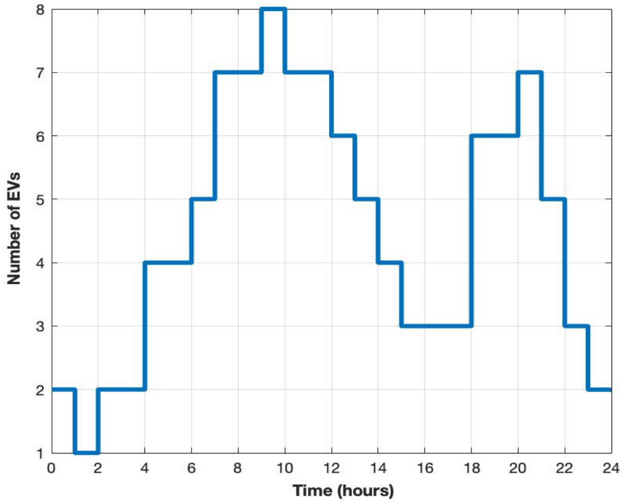

FIGURE 7. Total number of EVs connected to the system.

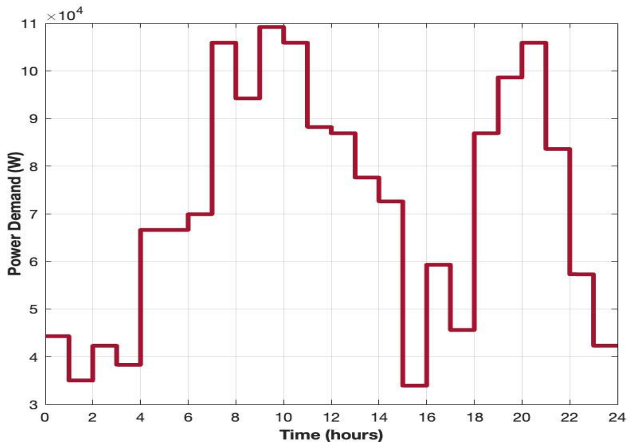

FIGURE 8. Total power demand.

The power demanded by the loads connected to nodes 3, 6, and 33 was 20 kW and remained constant throughout the day. The total power demand over the course of the day is shown in Figure 8 (step 4, Algorithm 1). The total power demand is the sum of the demand from the EVCS, other connected loads and the transmission losses in the system. The total power demand fluctuated, with the highest values observed between 6 to 12 hours and 18 to 22 hours.

The grid meets the demand that cannot be satisfied by renewable power generation. The excess power generated was fed back to the grid, as indicated by the negative values. The power across the point of common coupling, that is, the point of connection between the grid and the rest of the system is depicted in Figure 9.

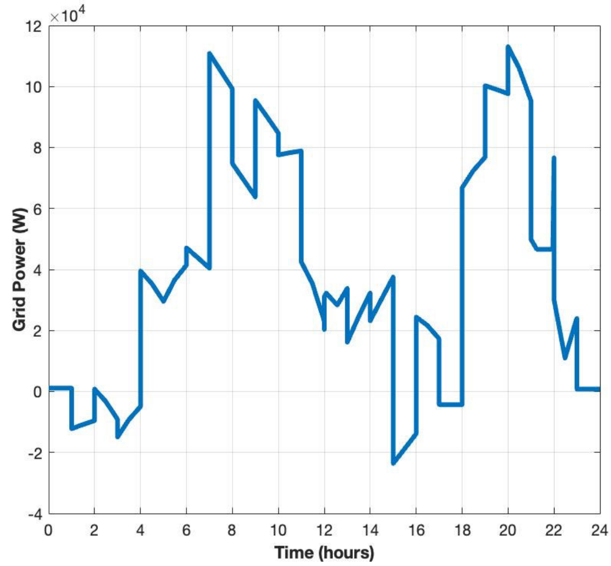

FIGURE 9. Power across the point of common coupling.

C. RENEWABLE UTILIZATION

The percentage of renewable energy utilization throughout the day is shown in Figure 10. This indicates the percentage of the power contribution of the renewable sources when compared to the total power obtained. An average of 68.94% of renewable power was used throughout the day.

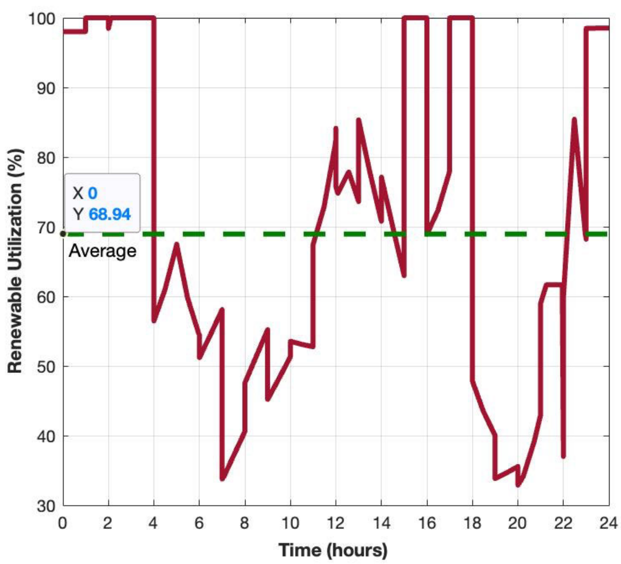

FIGURE 10. Renewable utilization.

D. DYNAMIC PRICING SCHEME

The cost per kWh to be paid by EV owners if the grid tariff is applied to the EVCS is shown in Figure 11. This corresponds to the TOD tariff shown in Table 4 of Section IV. In this case, the consumer pays an average of Rs. 6.579 per kWh.

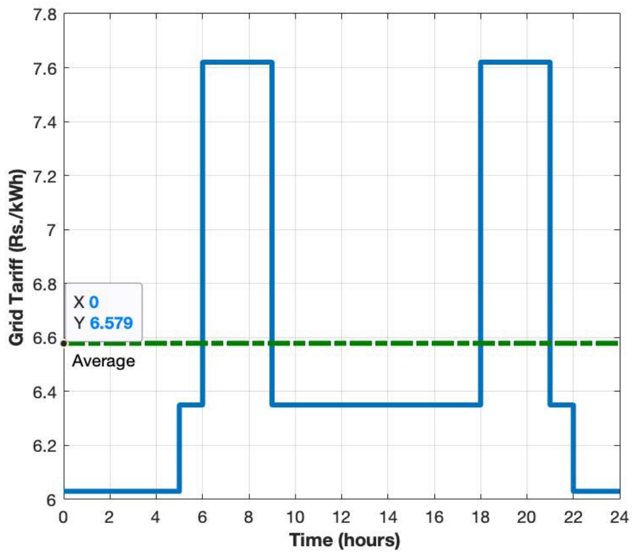

FIGURE 11. Time of day grid tariff.

The dynamic pricing scheme obtained using non-linear programming and the metaheuristic algorithms, according to the steps of Algorithm 1, is presented below.

1) DYNAMIC PRICING SCHEME – NON-LINEAR PROGRAMMING

The per-kWh cost determined using non-linear programming, based on the interior point algorithm, is shown in Figure 12. The upper and lower bounds specified in Table 3 were used as constraints for this method.

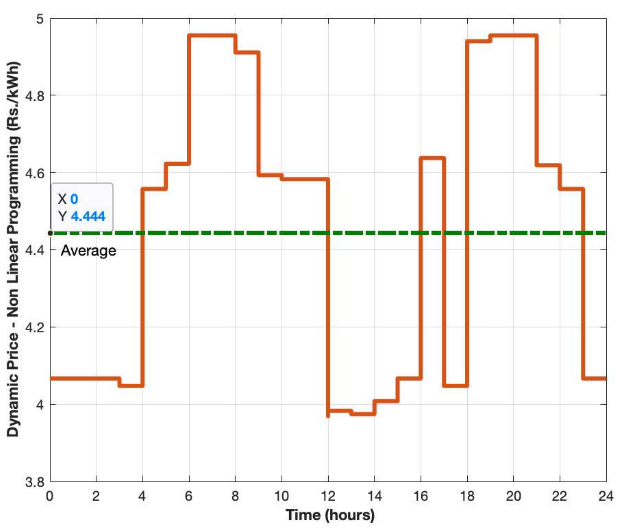

FIGURE 12. Dynamic pricing scheme – non-linear programming.

Consider the time interval of 0 to 6 hours. The power demand during this time was between 35 kW and 66.6 kW. On the other hand, the power generated by the renewables lies between 49.39 kW and 61.22 kW. Because the solar power is zero at this time, a per-unit cost of S_1, as shown in Table 3, is considered for the solar PV system. However, the wind profile varied between 4 kW and 15 kW. Thus the per-unit cost of the wind system may be W_1 or W_2, depending on the instantaneous power profile. The consumer pays an average of Rs. 4.444 per kWh over the 24 hour period, when non-linear programming is used.

2) DYNAMIC PRICING SCHEME – PSO

To perform optimization, 50 swarms were considered. The minimum and maximum inertia weights were assumed to be 0.3 and 0.8. The acceleration factors were assumed to be 2 and 2.01, respectively. The per kWh cost determined using PSO is shown in Figure 13.

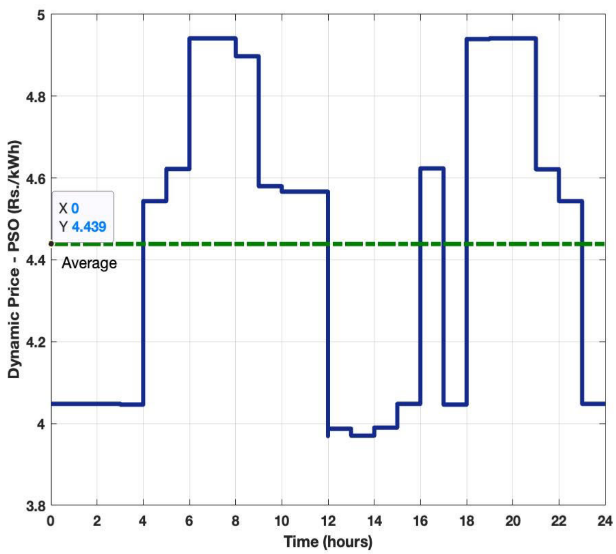

FIGURE 13. Dynamic pricing scheme – PSO.

Consider the time interval of 6 to 12 hours. The power demand during this time lies between 66.6 kW and 109.2 kW. On the other hand, the power generated by the renewables lies between 49.39 kW and 107.7 kW. Because the solar power and the wind power generations vary over the complete range specified in Table 3, the per-unit costs of the systems would change depending on the instantaneous power profile. The grid tariff is included in the calculation of the dynamic pricing scheme when the demand is not met by the renewable energy generation. The consumer pays an average of Rs. 4.439 per kWh over the 24 hour period, when PSO is used.

3) DYNAMIC PRICING SCHEME – SGO

To perform the optimization, a group of 50 people was considered. The self-introspection factor was assumed to be 0.7. The per-kWh cost determined using the SGO is shown in Figure 14.

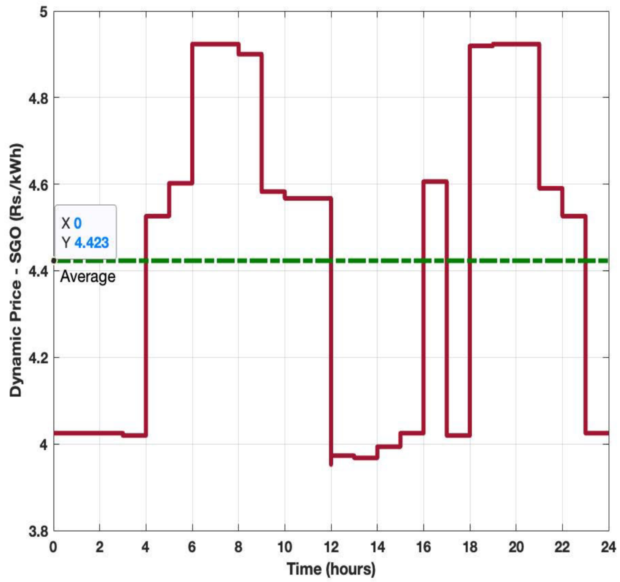

FIGURE 14. Dynamic pricing scheme – SGO.

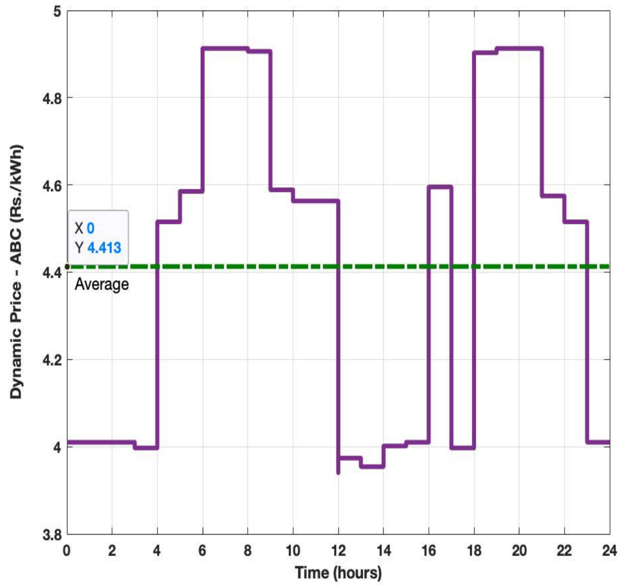

FIGURE 15. Dynamic pricing scheme – ABC.

Consider the time interval of 12 to 18 hours. The power demand during this time lies between 33.9 kW and 86.9 kW. In contrast, the power generated by the renewables lies between 54.05 kW and 99.67 kW. Because the solar power and the wind power generations vary over the complete range specified in Table 3, the per-unit costs of the systems would change depending on the power profile at a particular instant of time. The grid tariff is included in the calculation of the dynamic pricing scheme when the demand is not met by the renewable energy generation. The consumer pays an average of Rs. 4.423 per kWh over the 24 hour period, when SGO is used.

4) DYNAMIC PRICING SCHEME – ABC ALGORITHM

To perform the optimization, 100 food sources and 50 honey-bees were considered. The per kWh cost determined using the ABC algorithm is shown in Figure 15. In the duration between 18 and 24 hours, the power demand lies between 42.3 kW and 105.9 kW. However, the power generated by the renewables was between 45 and 75 kW. Because the solar power is zero in this duration, S1 is considered as the per-unit cost for the solar system. However, the wind profile varied over the complete range specified in Table 3. Thus the per-unit cost for the wind system may be W_1, W_2 or W_3, depending on the instantaneous power profile. The grid tariff is included in the calculation of the dynamic pricing scheme when the demand is not met by the renewable energy generation. The consumer pays an average of Rs. 4.413 per kWh over the 24 hour period, when the ABC algorithm is used.

A comparison of the results obtained using the different algorithms is presented in Table 5. If consumers are charged using the time-of-day grid tariff, they pay an average of Rs.6.579 per kWh. In contrast, they pay lesser per kWh in the case of the proposed dynamic pricing scheme. The average per unit costs obtained from the non-linear programming, PSO, SGO and ABC algorithms were Rs. 4.444, 4.439, 4.423 and 4.413, respectively. The ABC algorithm proved to be the most beneficial in terms of cost.

TABLE 5. Dynamic pricing scheme.

Scheme	Charging Cost (Rs./kWh)		
	Average	Minimum	Maximum
Time of Day Grid Tariff	6.579	6.03	7.62
Non-Linear Programming	4.444	3.969	4.955
PSO	4.439	3.939	4.941
SGO	4.423	3.952	4.924
ABC	4.413	3.94	4.913

The computational efficiency of the algorithms was tested using an Apple M2 chip with 8 core GPU and 8 GB RAM. In terms of computational efficiency, the metaheuristic algorithms performed better than non-linear programming (17.54 seconds). Among the metaheuristic algorithms, the SGO and ABC algorithms required similar times of 11.78 seconds and 11.66 seconds, respectively. They were quicker than PSO, that took 16.29 seconds for the same initial conditions.

Hence, the ABC algorithm is the best method for this application in terms of cost as well as computational time. If the generated power and demand are changed, the algorithm continues to provide the best possible cost.

E. PAYBACK PERIOD

The time required to repay the cost of the original investment on a project is called the payback period [36]. A lower payback period indicated a more feasible project. The payback period (PBP) may be given by

$$PBP = \frac{\text{Investment Cost}}{\text{Annual Revenue}} \text{years} \tag{17}$$

TABLE 6. Payback period for the renewable sources.

System	Rating (kW)	Instalment Cost (Rs.)	Operation and Maintenance Cost (Rs.)	Generated Energy (units/year)	Annual Revenue (Rs.)	Payback period (years)
Solar PV	35	1984500	70000	51100	321930	6.3818
Wind	30	1350000	3300	66000	415800	3.2546
Biogas	45	100000	2000	24637.5	155216.25	0.6571

The payback period was evaluated for each renewable source based on their ratings, as listed in Table 6. The payback periods obtained for the solar PV system, wind farm and biogas plant were 6.4 years, 3.3 years and 0.66 year respectively.

F. GREENHOUSE GAS (GHG) EMISSIONS

The GHG emissions from each renewable source were calculated based on their respective ratings, as shown in Table 7. The solar PV system did not release GHGs during operation. The wind farm contributes approximately 726 kilograms (kgs) of GHGs annually. The biogas plant contributes approximately 6159.4 kgs of GHGs per annum. For the same amount of energy obtained from renewables, a coal power plant emits 138902.8 kgs of GHGs.

TABLE 7. Estimated ghg emissions for the renewable sources.

System	Rating (kW)	GHG Emission (kg)/kWh	Generated Energy (units/year)	Total GHG /year (in kg)
Solar PV	35	0	51100	0
Wind	30	0.011	66000	726
Biogas	45	0.25	24637.5	6159.375
Total GHG Emission / year from renewable sources				6885.375
Thermal Power Station	100	0.98	141737.5	138902.75

G. THE MAIN DIFFERENCES BETWEEN THE PROPOSED AND EXISTING WORK

The proposed work is compared with the existing research in Table 8. The developed system is superior in the following respects:

[1] The modelled EVCS considers both AC and DC charging.
[2] The EMS was implemented in SCADA using meta-heuristic algorithms, thereby making the system more robust and reliable.
[3] Three renewable sources were considered for the system: solar, wind and biogas.

TABLE 8. Main differences between the proposed work and existing research.

Reference, Year	Proposed System	Method	Contribution
Ahmad et al. (2019)	EMS for public EVCS integrated with the community microgrid	Switching mechanism from one trading market to another	Minimizes the charging cost and meets the community load
Kouka et al. (2020)	EMS for a residential EVCS with a PV power source and an ESS	1) Power allocation and charging based on vehicle type	1) Stand-alone EVCS and optimized PV power use
Himabindu et al. (2021)	Optimal configuration (OC) and investment efficiency (IE) for solar powered EVCS for four Indian cities	1) Theoretical demand model and a stochastic model for EV traffic and a resource utilization pattern	1) OC and IE depend on the solar irradiation and the feed-in-tariff price of rooftop solar power in urban areas
Himabindu et al. (2023)	A biogas–solar powered EVCS for a typical location in Karnataka	1) Techno-economic assessment and environmental analysis was carried out	1) Dependency on the grid reduced with improved environment benefits in terms of carbon dioxide emissions
Karmaker et al. (2023)	A hybrid biogas and solar grid connected EVCS system with residential loads in Bangladesh	1) Optimization using fuzzy-logic based algorithm	1) Charging costs compared with flat rate tariff 2) Hours with lower charging cost proposed
Proposed Work (2024)	EMS for EVCS in a modified IEEE 33 bus system integrated with solar, biogas and wind systems	1) Dynamic Pricing Scheme based on Time of Day Tariff, charging duration, power generation and power demand. 2) Techno-economic assessment was also performed	1) Minimizes charging cost and maximizes the renewable energy utilization. 2) Payback period and GHG emissions are evaluated for the renewable sources

[4] Techno economic assessment of the developed system is made.

VI. CONCLUSION

With growing concerns about climate change and increased pollution, the transition to EVs and the integration of renewable sources in the power system has proven to be an effective method to curb the ill effects on the environment. This study deals with the development of a metaheuristic algorithm-based Energy Management System for an IEEE 33 bus system incorporated with an EVCS. Three renewable sources, namely, a solar PV system, a wind farm and a biogas plant were considered. A dynamic pricing scheme was developed to ensure that consumers pay a lower average price for EV charging, through the MAEMS in the SCADA master unit. Furthermore, the payback period and GHG emissions associated with the proposed system were estimated.

The ABC algorithm proved to be the most beneficial method, with the lowest average per-unit charging cost and the highest computational efficiency. The proposed scheme using the ABC algorithm is 32.92% more cost efficient than the conventional case. The average renewable energy utilization of the proposed model was approximately 68.94%. The modelled system saw an approximately 95% reduction in GHG emissions, when compared to its coal-powered counterpart.

Thus, the developed MAEMS achieves minimization of charging costs and maximization of renewable energy utilization. The reduced GHG emissions and favorable payback periods highlight the benefits of incorporating renewable sources into power systems.

REFERENCES

[1] A. G. Olabi and M. A. Abdelkareem, "Renewable energy and climate change," *Renew. Sustain. Energy Rev.*, vol. 158, no. 1, pp. 1–24, 2022.

[2] F. Perera and K. Nadeau, "Climate change, fossil-fuel pollution, and children's health," *New England J. Med.*, vol. 386, no. 24, pp. 2303–2314, Jun. 2022.

[3] M. Muratori, M. Alexander, D. Arent, M. Bazilian, P. Cazzola, E. M. Dede, J. Farrell, C. Gearhart, D. Greene, A. Jenn, M. Keyser, T. Lipman, S. Narumanchi, A. Pesaran, R. Sioshansi, E. Suomalainen, G. Tal, K. Walkowicz, and J. Ward, "The rise of electric vehicles—2020 status and future expectations," *Prog. Energy*, vol. 3, no. 2, Mar. 2021, Art. no. 022002.

[4] M. H. Ghodusinejad, Y. Noorollahi, and R. Zahedi, "Optimal site selection and sizing of solar EV charge stations," *J. Energy Storage*, vol. 56, Dec. 2022, Art. no. 105904.

[5] G. Krishna, "Understanding and identifying barriers to electric vehicle adoption through thematic analysis," *Transp. Res. Interdiscipl. Perspect.*, vol. 10, Jun. 2021, Art. no. 100364.

[6] A. Golder and S. S. Williamson, "Energy management systems for electric vehicle charging stations: A review," in *Proc. 48th Annu. Conf. IEEE Ind. Electron. Soc.*, Oct. 2022, pp. 1–6.

[7] K. Kouka, A. Masmoudi, A. Abdelkafi, and L. Krichen, "Dynamic energy management of an electric vehicle charging station using photovoltaic power," *Sustain. Energy, Grids Netw.*, vol. 24, Dec. 2020, Art. no. 100402.

[8] H. N., S. Hampannavar, D. B., and S. M., "Analysis of microgrid integrated photovoltaic (PV) powered electric vehicle charging stations (EVCS) under different solar irradiation conditions in india: A way towards sustainable development and growth," *Energy Rep.*, vol. 7, pp. 8534–8547, Nov. 2021.

[9] F. Ahmad, M. S. Alam, S. M. Shariff, and M. Krishnamurthy, "A cost-efficient approach to EV charging station integrated community microgrid: A case study of Indian power market," *IEEE Trans. Transport. Electrific.*, vol. 5, no. 1, pp. 200–214, Mar. 2019.

[10] K.-Y. Wu, T.-C. Tai, B.-H. Li, and C.-C. Kuo, "Dynamic energy management strategy of a solar-and-energy storage-integrated smart charging station," *Appl. Sci.*, vol. 14, no. 3, p. 1188, Jan. 2024.

[11] H. N., S. Hampannavar, D. B., O. M. Longe, S. Mansani, and V. Komanapalli, "Assessment of microgrid integrated biogas–photovoltaic powered electric vehicle charging station (EVCS) for sustainable future," *Energy Rep.*, vol. 9, pp. 139–143, Nov. 2023.

[12] M. M. Rahman, E. A. Al-Ammar, H. S. Das, and W. Ko, "Optimal design of grid connected PV battery system for probabilistic EVCS load," in *Proc. Adv. Sci. Eng. Technol. Int. Conf. (ASET)*, Feb. 2020, pp. 1–6.

[13] S. Hussain, M. A. Ahmed, K.-B. Lee, and Y.-C. Kim, "Fuzzy logic weight based charging scheme for optimal distribution of charging power among electric vehicles in a parking lot," *Energies*, vol. 13, no. 12, p. 3119, Jun. 2020.

[14] A. K. Karmaker, Md. A. Hossain, H. R. Pota, A. Onen, and J. Jung, "Energy management system for hybrid renewable energy-based electric vehicle charging station," *IEEE Access*, vol. 11, pp. 27793–27805, 2023.

[15] P. Roy, J. He, T. Zhao, and Y. V. Singh, "Recent advances of wind-solar hybrid renewable energy systems for power generation: A review," *IEEE Open J. Ind. Electron. Soc.*, vol. 3, pp. 81–104, 2022.

[16] M. Z. Malik, K. Zehra, I. Ali, Ubedullah, M. Ismail, A. Hussain, V. Kumar, M. Abid, and M. H. Baloch, "Solar-wind hybrid energy generation system," in *Proc. IEEE 23rd Int. Multitopic Conf. (INMIC)*, Nov. 2020, pp. 1–6.

[17] A. N. Celik, "Optimisation and techno-economic analysis of autonomous photovoltaic-wind hybrid energy systems in comparison to single photo-voltaic and wind systems," *Energy Convers. Manage.*, vol. 43, no. 18, pp. 2453–2468, Dec. 2002.

[18] M. S. Alam and S. A. Arefifar, "Energy management in power distribution systems: Review, classification, limitations and challenges," *IEEE Access*, vol. 7, pp. 92979–93001, 2019.

[19] Y. Zahraoui, I. Alhamrouni, S. Mekhilef, M. R. B. Khan, M. Seyedmahmoudian, A. Stojcevski, and B. Horan, "Energy management system in microgrids: A comprehensive review," *Sustainability*, vol. 13, no. 19, p. 10492, Sep. 2021.

[20] R. K. Chauhan, M. L. Dewal, and K. Chauhan, "Intelligent SCADA system," *Int. J. Power Syst. Optim. Control*, vol. 2, no. 1, pp. 143–149, Jan. 2010.

[21] A. J. Calderón Godoy and I. González Pérez, "Integration of sensor and actuator networks and the SCADA system to promote the migration of the legacy flexible manufacturing system towards the Industry 4.0 concept," *J. Sensor Actuator Netw.*, vol. 7, no. 2, p. 23, May 2018.

[22] D. K. Mohanta and J. B. Reddy, *Synchronized Phasor Measurements for Smart Grids*, document 137836, 2017.

[23] Y. D. Shahakar and D. A. Shahakar, "Introduction and classification of classical and advanced optimization methods for electric power system," in *Proc. Int. Conf. Innov. Trends Adv. Eng. Technol.*, Dec. 2019, pp. 53–59.

[24] C. L. B. Silveira, A. Tabares, L. T. Faria, and J. F. Franco, "Mathematical optimization versus metaheuristic techniques: A performance comparison for reconfiguration of distribution systems," *Electr. Power Syst. Res.*, vol. 196, Jul. 2021, Art. no. 107272.

[25] W. Wong and C. I. Ming, "A review on metaheuristic algorithms: Recent trends, benchmarking and applications," in *Proc. 7th Int. Conf. Smart Comput. Commun. (ICSCC)*, Jun. 2019, pp. 1–5.

[26] D. Wang, D. Tan, and L. Liu, "Particle swarm optimization algorithm: An overview," *Soft Comput.*, vol. 22, no. 2, pp. 387–408, Jan. 2017.

[27] A. G. Gad, "Particle swarm optimization algorithm and its applications: A systematic review," *Arch. Comput. Methods Eng.*, vol. 29, no. 5, pp. 2531–2561, Apr. 2022.

[28] S. Satapathy and A. Naik, "Social group optimization (SGO): A new population evolutionary optimization technique," *Complex Intell. Syst.*, vol. 2, no. 3, pp. 173–203, Aug. 2016.

[29] Y. Xu, P. Fan, and L. Yuan, "A simple and efficient artificial bee colony algorithm," *Math. Problems Eng.*, vol. 2013, pp. 1–9, Aug. 2013.

[30] K. R. Guerriche and T. Bouktir, "Maximum loading point in distribution system with renewable resources penetration," in *Proc. Int. Renew. Sustain. Energy Conf. (IRSEC)*, Ouarzazate, Morocco, Oct. 2014, pp. 481–486.

[31] A. Gautam, R. Shukla, K. Kishore, P. Jain, R. K. Porwal, and N. Nallarasan, "Analyses of Indian power system frequency," in *Proc. IEEE Int. Conf. Power Syst. Technol. (POWERCON)*, Sep. 2020, pp. 1–6.

[32] (2021). *Handbook of Electric Vehicle Charging Infrastructure Implementation*. [Online]. Available: https://www.niti.gov.in/sites/default/files/2021-08/HandbookforEVChargingInfrastructureImplementation081221.pdf

[33] S. K. Sahu, S. Kumar, D. Ghosh, and S. Poddar, "Modelling and analysis of distribution system performance with integration of electric vehicle charging station in real-time environment," in *Proc. IEEE 18th India Council Int. Conf. (INDICON)*, Guwahati, India, Dec. 2021, pp. 1–6.

[34] A. K. Singh and A. H. Idrisi, "Evolution of renewable energy in India: Wind and solar," *J. Inst. Eng. (India), Ser. C*, vol. 101, no. 2, pp. 415–427, Nov. 2019.
[35] (2019). *Report on Time of Day (TOD) Tariff For Tangedco*. Accessed: Jul. 12, 2024. [Online]. Available: http://www.tnerc.gov.in/PressRelease/files/PR-230820220439Eng.pdf
[36] M. Gjelaj, C. Træholt, S. Hashemi, and P. B. Andersen, "Cost-benefit analysis of a novel DC fast-charging station with a local battery storage for EVs," in *Proc. 52nd Int. Universities Power Eng. Conf. (UPEC)*, Aug. 2017, pp. 1–6.

JENNIE ANGELA JOSE SHIRLEY (Student Member, IEEE) was born in India, in 2003. She is currently pursuing the B.Tech. degree in electrical and electronics engineering with the National Institute of Technology (NIT) Tiruchirappalli, Tiruchirappalli, India.

She interned at Jyoti Sohar Switchgear LLC, Oman, and Voltamp Power Oman, in 2022. Her research interests include smart grids, wide-area monitoring systems, electric vehicles, and high-voltage technology.

Ms. Jose Shirley was awarded the DAAD WISE Scholarship, in 2023, for a research internship at the University of Stuttgart, Germany.

R. P. POOJA is currently pursuing the B.Tech. degree in electrical and electronics engineering with the National Institute of Technology (NIT) Tiruchirappalli, Tiruchirappalli, India.

She underwent an internship at leading multinational consultancies, including Petrofac and Technip Energies, India, in 2023. She has published one journal article in a well-recognized high-quality journal. Her research interests include energy management systems, machine learning, electric vehicle technologies, embedded systems, power system technologies, green energies, and power electronics.

MADDIKARA JAYA BHARATA REDDY (Senior Member, IEEE) was born in India, in 1980. He received the B.Tech. degree in electrical and electronics engineering from Acharya Nagarjuna University, Guntur, India, in 2002, and the M.E. degree in electrical engineering and the Ph.D. degree from the Birla Institute of Technology (BIT), Ranchi, India, in 2004 and 2008, respectively.

He has 20 years of experience in teaching and research. He is currently a Professor with the Department of Electrical and Electronics Engineering, National Institute of Technology (NIT) Tiruchirappalli, Tiruchirappalli, India. His current research interests include smart grids, substation automation, wide-area protection, digital relaying, soft computing applications in power systems, and power system protection.

Dr. Reddy is an Editor of the *Electric Power Components and Systems* (Taylor & Francis Publications) and a Subject Editor of *IET Generation, Transmission & Distribution*.